HHS Public Access

Author manuscript

Nat Neurosci. Author manuscript; available in PMC 2009 May 01.

Published in final edited form as:

Nat Neurosci. 2008 November ; 11(11): 1294–1301. doi:10.1038/nn.2210.

Focal Transplantation-based Astrocyte Replacement is Neuroprotective in a Model of Motor Neuron Disease

Angelo C. Lepore[1], **Britta Rauck**[1], **Christine Dejea**[1], **Andrea C. Pardo**[1], **Mahendra S. Rao**[3], **Jeffrey D. Rothstein**[1,2], and **Nicholas J. Maragakis**[1,4]

[1]Department of Neurology, The Johns Hopkins University School of Medicine, 600 N. Wolfe St., Meyer 6-109, Baltimore, MD 21287

[2]Department of Neuroscience, The Johns Hopkins University School of Medicine, 600 N. Wolfe St., Meyer 6-109, Baltimore, MD 21287

[3]Invitrogen Corporation, 1610 Faraday Ave, Carlsbad, CA 92008

Abstract

Cellular abnormalities in amyotrophic lateral sclerosis (ALS) are not limited to motor neurons. Astrocyte dysfunction occurs in human ALS and SOD1^{G93A} animal models. Therefore, the value of focal enrichment of normal astrocytes was investigated using transplantation of lineage-restricted astrocyte precursors, Glial-Restricted Precursors (GRPs). GRPs were transplanted around cervical spinal cord respiratory motor neuron pools, the principal cells responsible for death in this neurodegenerative disease. GRPs survived in diseased tissue, differentiated efficiently into astrocytes, and reduced microgliosis in SOD1^{G93A} rat cervical spinal cord. GRPs extended survival and disease duration, attenuated motor neuron loss, and slowed declines in fore-limb motor and respiratory physiological function. Neuroprotection was mediated in part by the primary astrocyte glutamate transporter, GLT1. These findings demonstrate the feasibility and efficacy of transplantation-based astrocyte replacement, and show that targeted multi-segmental cell delivery to cervical spinal cord is a promising therapeutic strategy for slowing focal motor neuron loss associated with ALS.

Keywords

stem cell; grafting; transplantation; motor neuron; neurodegeneration; replacement; neuroprotection; non-cell autonomous; astroglia; astrocyte; neural precursor cell; progenitor; lineage-restricted precursor; glial precursor; ALS; amyotrophic lateral sclerosis; SOD1

[4]To whom correspondence should be addressed: Nicholas J. Maragakis, M.D., Department of Neurology, The Johns Hopkins School of Medicine, 600 North Wolfe Street, Meyer 6-119, Baltimore, MD 21287, Phone: 410-614-9874, Fax: 443-287-3933, E-mail: nmaragak@jhmi.edu.

Author Contributions

A.C.L. designed and conducted the experiments, analyzed the data, prepared the figures, and wrote the manuscript. N.J.M. supervised the project, and participated in designing experiments and writing the manuscript. M.S.R. and J.D.R. participated in designing experiments and writing the manuscript. B.R., A.C.P. and C.D. conducted experiments.

Potential Conflict of Interest

M.S.R. works for Invitrogen Corporation, which is a supplier of reagents to the stem cell research community.

Amyotrophic lateral sclerosis (ALS), a motor neuron disorder that affects approximately 30,000 individuals in the U.S. alone, is characterized by a relatively rapid degeneration of upper and lower motor neurons, with death normally occurring 2–5 years following diagnosis due to respiratory failure1. The vast majority of cases are sporadic, and 5–10% are familial (fALS), with 20% of familial cases linked to mutations in the Cu/Zn superoxide dismutase 1 (SOD1) gene2. Transgenic mice3–5 and rats6 carrying mutant human SOD1 genes$^{(G93A, G37R, G86R, G85R)}$ recapitulate many, although not all, features of the human disease.

Despite the relative selectivity of motor neuron cell death, animal and tissue culture models of fALS suggest that non-neuronal cells contribute significantly to neuronal dysfunction and death7–13. CNS astrocytes outnumber their neuronal counterparts approximately ten-fold, and play crucial roles in adult CNS homeostasis14, including the vast majority of synaptic glutamate uptake15,16, maintenance of extracellular potassium, and nutrient support of neurons. Multiple properties of spinal cord and brain astrocytes are compromised in ALS, and these changes often precede clinical disease onset17. Initial evidence for an astroglial contribution to ALS came from studies of both humans and rodent ALS models demonstrating dysfunction and large decreases in levels of the primary astrocyte glutamate transporter, GLT1 (EAAT2 in the human), in areas of motor neuron loss6,18. Confirmation of a role for non-neuronal cells came from recent studies of chimeric animals demonstrating that glia can modulate mutant SOD1-induced pathological changes in neighboring motor neurons8. These studies highlight the important role played by astrocyte-motor neuron interactions in the etiology of ALS.

Regardless of whether astrocyte dysfunction is the cause of disease or a consequence of neuronal death, altered physiology of pathologic astrocytes results in further susceptibility to motor neuron loss and contributes to disease progression. We hypothesized that replacement or enrichment with healthy astrocytes, employing transplantation of Glial-Restricted Precursors (GRPs)19,20 - lineage-restricted astrocyte precursors derived from developing spinal cord, could be a therapeutic approach for slowing and/or halting disease course. Such an approach would lend itself to reconstituting a more normal astrocytic environment in the spinal cord. This may include, for example, restoration of extracellular glutamate homeostasis by preventing ALS-associated loss of GLT1. In humans with ALS (and mutant SOD1 animals), patients ultimately succumb to disease because of respiratory compromise due to loss of phrenic motor neuron innervation of the diaphragm21,22. In order to target therapy to diaphragmatic function, GRPs were transplanted into cervical spinal cord ventral gray matter of SOD1^{G93A} rats. Because this approach would aim towards neuroprotection rather than neuronal replacement, reconstitution of spinal cord astrocytes may be a valuable approach to cellular based therapeutics.

Results

To assess the phenotypic effect of GRP transplantation, GRPs were transplanted into the cervical spinal cord of 90 day old SOD1^{G93A} rats. Because diaphragm function is the primary cause of death in ALS patients and rodent models21,22, the transplantation strategy

in this study targeted respiratory motor neurons that innervate diaphragm via bilateral cell injections at cervical spinal cord levels 4, 5 and 6.

Robust Transplant Survival in SOD1^{G93A} Cervical Spinal Cord

GFP$^+$ GRPs were transplanted into the cervical spinal cord of SOD1^{G93A} rats (n = 34) at 90 days of age. Despite ongoing disease progression, GRPs robustly survived in gray (Fig. 1a–b) and white (Fig. 1b) matter regions of cervical spinal cord at disease end-stage, up to 80 days post-transplantation. A total of 9.0×10^5 cells were grafted into each animal (6 sites; 1.5×10^5 cells/site). Six discrete sites with transplanted cells were found in animals. Quantification of the number of GFP$^+$ GRPs at end-stage revealed that 32.2 ± 4.6% of transplanted cells survived (n = 3). No damage to the spinal cord, including cyst formation, was detected when spinal cords from any of the groups (media, dead cells, fibroblasts, GRPs) were assessed with cresyl violet staining (not shown), and no sign of tumor formation was found in any animal.

The profile of graft proliferation was determined via double immunohistochemistry for GFP and the proliferation marker, Ki67 (Fig. 1c). Only a small percentage of cells continued to divide at 2 days post-transplantation (8.1 ± 2.1%; n = 3; Fig. 1d), while transplant-derived cells no longer proliferated at disease end-stage (0.6 ± 0.6%; n = 3; Fig. 1d). These results suggest that the robust survival of transplanted cells at disease end-stage was not a function of extensive early graft proliferation in vivo.

To assess whether transplantation of greater numbers of cells would result in enhanced graft survival, a nearly three fold increase in cells (4.0×10^5/site) was delivered to each site; however, this approach resulted in obvious necrotic tissue damage at the sites of injection.

No instances of GFP$^+$ transplanted cells co-labeled with human SOD1 were ever noted at disease end-stage, demonstrating that transplanted GFP$^+$ cells did not fuse with host cells (Fig. 1e).

Ventral Horn Localization and White Matter Migration

GRPs were specifically detected in the ventral horn (Fig. 1a), the region of ongoing degeneration. In addition, transplanted cells migrated extensively and selectively along surrounding white matter tracts in both rostral and caudal directions (Fig. 1b). Quantification of migration revealed that at 2 days post-engraftment, transplanted cells were found on average no farther than 0.19 ± 0.03mm from the injection site (n = 4; Fig. 1f), while GRPs had migrated up to 8.3 ± 0.95mm from the injection site at disease end-stage (n = 4). Histograms depicting the percentage of cells at various distances from sites of injection show that the migratory pattern of transplants in gray versus white matter was distinct. The vast majority of cells were located close to the injection site in gray matter (Fig. 1g). In white matter, the highest proportion of cells was located close to the injection, and the location of cells gradually tapered away with increased distance (Fig. 1h). Even though widely dispersed, the majority of transplanted cells still remained adjacent to the injection sites in both white and gray matter regions of the cervical spinal cord, and were not seen in more distant brain or spinal cord regions (not shown).

Efficient Astrocyte Differentiation

To assess differentiation of transplanted cells, double immunohistochemistry for GFP with specific markers of cell fate was employed. Initially following grafting, the vast majority of cells were still nestin$^+$ GRPs (85.4 ± 3.6%; Fig. 2a), with a small percentage of astrocytes constituting the remaining population (10.6 ± 7.5%). At end-stage, GRPs efficiently differentiated (87.9 ± 4.0%) into GFAP$^+$ astrocytes following transplantation (Fig. 2c–d). Quantification of the differentiation profile of transplanted GRPs at 2 days post-transplantation and at disease end-stage depicts the efficient transition from immature to mature phenotypes in vivo (n = 3; Fig. 2e). A small percentage of cells also differentiated into oligodendrocytes by end-stage (8.6 ± 0.35%), while no transplanted cells gave rise to unexpected phenotypes such as neurons, microglia, or macrophages. In addition, only a small percentage of cells remained as undifferentiated nestin$^+$ GRPs at end-stage (10.2 ± 6.9%), demonstrating that the majority of transplanted cells differentiated into mature phenotypes.

During the course of disease, graft-derived astrocytes elaborated mature astrocyte morphologies (Fig. 2b). These cells localized not only in the vicinity of host motor neurons in the ventral horn, but also spatially interacted with host motor neuron soma and dendritic fields. Confocal microscopy revealed that transplanted GRPs were closely apposed to cell bodies of ChAT$^+$ host motor neurons (Fig. 2f). These interactions can also be appreciated with 3-D reconstruction of confocal images showing GFP$^+$ cells 3-Dimensionally surrounding host ChAT$^+$ motor neurons (Supp. Video 1). Confocal imaging of GFP and the pre-synaptic marker, synapsin, also shows the localization of transplanted GFP$^+$ cells at synaptic sites within ventral gray matter (Fig. 2g).

Continued GLT1 Expression and Absence of Ubiquitin Aggregation

To determine if transplanted cells succumbed to a similar pathological fate as host astrocytes in response to disease, two characteristic pathological changes observed in host astrocytes in the spinal cord of SOD1^{G93A} animals, the presence of ubiquinated inclusions3,5 and the loss of GLT1 expression6, were examined. Extensive ubiquitin deposition was found in host cervical spinal cord motor neurons and astrocytes (not shown). As demonstrated by confocal microscopy at end-stage, the vast majority of transplanted GRP-derived cells did not contain ubiquitin aggregates (Fig. 2h). Only 6.1 ± 1.7% of GFP$^+$ cells containing such inclusions (n = 5). In addition, grafted cells continued to express the astrocyte glutamate transporter protein, GLT1, at end-stage (Fig. 4f).

Delayed Decline in Motor Function and Survival Extension

SOD1^{G93A} rats display a typical pattern of disease progression in which hind-limb onset precedes onset of disease in the fore-limbs, followed by animals reaching disease end-stage as a result of compromised respiratory function23. Transplants were delivered to cervical spinal cord, thereby focally targeting fore-limb and respiratory function, but not hind-limb motor neurons.

Because transplants were delivered to the location of respiratory motor neurons in cervical spinal cord, the ability to extend survival was assessed. Compared to media (n = 10) and

dead cell (n = 7) controls, GRPs (n = 10) increased overall animal survival by 16.9 days (media: 155.8 ± 12.0 days; dead cells: 155.8 ± 14.0; GRPs: 172.7 ± 14.1; $p < 0.05$: media vs. GRPs; $p < 0.01$: dead vs. GRPs; Fig. 3a).

GRP transplanted animals showed a trend towards an increase in fore-limb disease onset (media: 151.0 ± 12.0 days; dead cells: 149.3 ± 13.2; GRPs: 162.6 ± 11.9: $p > 0.05$; Fig. 3c); however, this change was not significant. No effect of GRPs on hind-limb disease onset was noted (media: 143.6 ± 12.3 days; dead cells: 142.2 ± 12.2; GRPs: 147.6 ± 12.9: $p > 0.05$; Fig. 3b).

Because transplants specifically targeted the cervical spinal cord, the ability to delay the regional progression of disease was examined. GRPs significantly delayed disease duration: the time between overall disease onset (i.e. hind-limb onset) and end-stage (media: 12.9 ± 3.3 days; dead cells: 14.7 ± 4.5; GRPs: 21.9 ± 6.1; $p < 0.001$: media vs. GRPs; $p < 0.05$: dead vs. GRPs; Fig. 3d). GRP transplants also significantly increased the delay to fore-limb disease onset following hind-limb onset (media: 7.4 ± 1.2 days; dead cells: 7.3 ± 3.1; GRPs: 14.9 ± 5.9; $p < 0.001$: media vs. GRPs; $p < 0.05$: dead vs. GRPs; Fig. 3e), suggesting that transplantation was able to focally interrupt disease progression from lumbar to cervical spinal cord. GRPs did not significantly delay weight decline ($p > 0.05$ for all comparisons; Fig. 3f).

The ability of GRP transplants to differentially affect fore-limb and hind-limb motor function was assessed via grip strength testing. GRPs had no effect on the rate of hind-limb grip strength decline ($p > 0.05$ for all comparisons; Fig. 3g), but significantly slowed decline in fore-limb grip strength ($p < 0.05$ at a number of time points following transplantation; Fig. 3h), suggesting that targeting transplantation to cervical spinal cord results in anatomically-specific effects. Transplants also slowed decline in motor performance (Fig. 3i).

Previous work demonstrated that seeding of GLT1 over-expressing GRPs on the organotypic slice culture model of motor neuron degeneration results in greater motor neuron preservation than wild-type GRPs, and this effect was mediated by enhanced glutamate uptake24. Therefore, the therapeutic efficacy of GLT1 over-expressing GRPs (G3s) relative to GRPs was examined in the present study. There were no significant differences between GRP (n = 10) and GLT over-expressing GRP (n = 9) transplants in disease duration (GRPs: 21.9 ± 6.1 days; GLT1 over-expressing GRPs: 22.8 ± 3.9; $p > 0.05$; Supp. Fig. 1a) or in delay to fore-limb disease onset following hind-limb onset (GRPs: 14.9 ± 5.9 days; GLT1 over-expressing GRPs: 15.4 ± 4.8; $p > 0.05$; Supp. Fig. 1b), two pertinent outcomes that were robustly enhanced by GRP transplantation compared to media and dead cell control groups.

Furthermore, GLT1-null GRPs were generated from $GLT1^{-/-}$ mice24 in order to test the role of graft-derived GLT1 in disease outcome. $GLT1^{-/-}$ GRPs were transplanted into $SOD1^{G93A}$ rat cervical spinal cord using the exact same approach as all other transplant groups. Unlike transplants of GRPs and GLT1 over-expressing GRPs, $GLT1^{-/-}$ GRPs (n = 8) did not extend disease duration (16.6 ± 2.0 days; Supp. Fig. 1a) or prolong the delay to

fore-limb disease onset following hind-limb onset (7.8 ± 1.4 days; Supp. Fig. 1b). To control for potential species differences in efficacy between rat (GRPs and GLT1 over-expressing GRPs) and mouse ($GLT1^{-/-}$ GRPs) -derived cell types, GRPs derived from wild-type mice (n = 6) were also transplanted. Similar to rat-derived GRPs and GLT1 over-expressing GRPs, wild-type mouse GRPs extended disease duration (22.4 ± 3.0 days; data not shown) and prolonged the delay to fore-limb disease onset following hind-limb onset (13.3 ± 3.1 days; data not shown). In addition, both wild-type and $GLT1^{-/-}$ mouse-derived GRPs survived (31.3% ± 0.07; Supp. Fig. 2a), differentiated into astrocytes (85.6 ± 1.3%; Supp. Fig. 2b) and migrated selectively along white matter tracts (5.7 ± 0.2 mm), as detected with the mouse-specific M2 antibody at disease endstage (n = 3; $GLT1^{-/-}$ GRPs). Quantification of these results showed that the fate of mouse-derived cells was very similar to the results presented earlier for rat-derived GRPs. These findings suggest that there was no significant species-related rejection of mouse-derived GRPs in the rat spinal cord. Combined with the efficacy seen with wild-type mouse GRP transplants, these findings suggest that the effects of $GLT1^{-/-}$ GRP transplantation were a function of a lack of GLT1, not due to a species-specific phenomenon.

Lastly, rat-derived fibroblasts25 were transplanted in order to test the effect of a non-neural live cell type on disease outcome (n = 6), as well as to control for the potential influence of immune-mediated clearing of dead transplanted cells. As demonstrated by immunofluorescence detection of the transplant marker, human placental alkaline phosphatase, fibroblast transplants survived in cervical spinal cord gray matter until disease end-stage in all rats (Supp. Fig. 1c–d). Disease duration (14.3 ± 0.8 days; Supp. Fig. 1b) and delay to fore-limb disease onset following hind-limb onset (5.8 ± 1.0 days; Supp. Fig. 1b) in $SOD1^{G93A}$ rats with fibroblasts transplants were not significantly different than media and dead cell controls.

Phrenic CMAPs and Cervical Motor Neuron Loss

Compared to age-matched wild-type rats (n = 3; 5.8 ± 0.7mV), all groups of $SOD1^{G93A}$ rats, regardless of experimental treatment, had significantly reduced peak response amplitudes in phrenic nerve compound muscle action potentials (CMAPs), a functional electrophysiological assay of diaphragm function21. Compared to media (n = 10) or dead cell (n = 8) controls, GRP (n = 8) transplantation slowed the decline in CMAP amplitudes. CMAPs (Fig. 4a–b) were recorded at 8 days post hind-limb disease onset, and a significant increase (Fig. 4c) in peak response amplitude was found in GRP transplanted rats (media: 2.25 ± 0.8mV; dead cells: 2.1 ± 0.6; GRPs: 3.2 ± 1.0; $p < 0.05$: media and dead cells vs. GRPs). Transplants had no effect on the response latency (media: 3.7 ± 0.1msec; dead cells: 3.6 ± 0.2; GRPs: 3.5 ± 0.2; $p > 0.05$; Fig. 4d).

The neuroprotective effect of GRPs on cervical spinal cord motor neuron loss was quantified. Compared to age-matched wild-type rats (n = 3; 18.5 ± 5.9 motor neurons/section; Fig. 4e), all groups of $SOD1^{G93A}$ rats, regardless of experimental treatment, had significantly reduced numbers of cervical spinal cord motor neurons. Compared to dead cell control (n = 9), GRPs (n = 5) partially rescued (a 47% increase) cervical motor neurons

(dead cells: 5.3 ± 2.0; GRPs: 7.8 ± 3.2; $p < 0.05$), likely accounting for the benefits observed in functional/behavioral measures.

No differences were noted between GRPs, GLT over-expressing GRPs, and wild-type mouse GRPs with respect to CMAP amplitudes (data not shown; GLT1 over-expressing GRPs (G3s): n = 5, 3.5 ± 0.3mV; wild-type mouse GRPs: n = 5; 3.4 ± 0.4mV; $p > 0.05$ for all comparisons) or between GRPs and GLT over-expressing GRPs with respect to cervical motor neuron counts (data not shown; GLT1 over-expressing GRPs: n = 4, 9.4 ± 2.0 motor neurons/section; $p > 0.05$).

Partial Preservation of Cervical Spinal Cord GLT1 Levels

Previous work has demonstrated the role played by loss of astroglial glutamate transport in the progression of ALS26. Preservation of GLT1 levels, either via transplant-derived replacement or prevention of loss from host cells, provides one possible mechanism for astrocyte-specific transplant efficacy. Therefore, levels of GLT1 protein in cervical spinal cord were measured at 8 days post hind-limb onset (Fig. 4g). Compared to age-matched wild-type rats (n = 2; 1.22 ± 0.23 arbitrary units; Fig. 4h), all groups of $SOD1^{G93A}$ rats, regardless of experimental treatment, had reduced levels of total GLT1 protein at the C4 cervical spinal cord level. Transplantation of GRPs attenuated the loss of total GLT1 levels focally in the spinal cord at C4 (n = 3/group; dead cells: 0.32 ± 0.09; GRPs: 0.84 ± 0.23; $p < 0.05$; Fig. 4h) and C6 levels (not shown). No differences amongst treatment groups in levels of total GLT1 were found when lumbar level 5 (L5) tissue was tested (wild-type: n = 2, 1.36 arbitrary units ± 0.50; dead cells: n = 5, 0.26 ± 0.18; GRPs: n = 5, 0.17 ± 0.11; $p > 0.05$: dead vs. GRPs; Fig. 4h), although all $SOD1^{G93A}$ rat groups had reduced levels compared to age-matched wild-type rats.

Notably, although GLT1 over-expressing GRPs have much higher expression levels of GLT1 in vitro compared to GRPs24, total GLT1 levels in C4 spinal cord transplanted with GLT1 over-expressing GRPs were not significantly higher compared to GRP transplanted tissue (n = 3; 0.95 ± 0.12 arbitrary units; GLT1 over-expressing GRPs vs. GRPs: $p > 0.05$; Fig. 4h). Unlike transplants of GRPs and GLT1 over-expressing GRPs, $GLT1^{-/-}$ GRPs (n = 3) did not maintain GLT1 expression. There was no significant difference in levels of GLT1 in cervical spinal cord between dead cell controls and $GLT1^{-/-}$ GRP transplants ($GLT1^{-/-}$ GRPs: n = 3; 0.33 ± 0.17 arbitrary units; $GLT1^{-/-}$ GRPs vs. GRPs: $p < 0.05$; $GLT1^{-/-}$ GRPs vs. dead cells: $p > 0.05$; Fig. 4h). These results suggest that graft-derived GLT1 accounts for most of the preservation of cervical spinal cord GLT1 levels following transplantation. Taken together, these results provide at least one plausible benefit of astrocyte replacement, although other astrocytic mechanisms may also be relevant as well.

No Changes in Cervical Spinal Cord Growth Factor Levels

GRP transplants may also have promoted therapeutic benefit via mechanisms other than increased GLT1 levels. For example, GRP transplants could release trophic factors, resulting in neuroprotection. ELISA was conducted on cervical spinal cord parenchyma at the levels of GRP transplantation to examine levels of BDNF, IGF-1, and VEGF. The beneficial roles of these particular trophic factors on disease outcome in mutant SOD1-expressing rodent

models have been previously shown27. Significant differences in levels of VEGF (wild-type: 46.3 ± 15.2pg/mL; dead cells: 48.1 ± 1.3; GRPs: 61.9 ± 11.2; n = 3/group; $p > 0.05$ for all comparisons; Supp. Fig. 3a), BDNF (wild-type: 3.6 ± 0.7pg/mL; dead cells: 5.8 ± 1.7; GRPs: 4.6 ± 1.2; n = 3/group; $p > 0.05$ for all comparisons; Supp. Fig. 3b) or IGF-1 (wild-type: 142.6 ± 29.8pg/mL; dead cells: 150.7 ± 23.9; GRPs: 172.1 ± 18.7; n = 3/group; $p > 0.05$ for all comparisons; Supp. Fig. 3c) were not observed between any of the groups studied.

Decreased Ventral Horn Microgliosis

The inflammatory response was examined with the microglial marker, Iba1, in age-matched cervical spinal cord from media and GRP-transplanted animals. Immunohistochemistry revealed that compared to wild-type spinal cord (Fig. 5a; n = 4), there was a significantly elevated microglial response specifically in the ventral gray matter of both media control (n = 6; Fig. 5b) and GRP transplanted (n = 4; Fig. 5c) $SOD1^{G93A}$ rat groups. However, the response was significantly reduced in GRP transplanted animals (Fig. 5d; wild-type: 58.0 ± 4.1 arbitrary units; media: 110.0 ± 3.4; GRPs: 95.4 ± 2.8; $p < 0.05$). The present effects of GRP transplantation on disease progression following symptomatic onset are similar to the previous results7 in which mutant SOD1 expression was selectively removed from microglia, and may in part be attributed to a muted microglial response in cervical spinal cord.

Discussion

The neuroprotective effects observed in this study demonstrate the feasibility and efficacy of focal transplantation-based astrocyte replacement for ALS and also show that targeted multi-segmental cell delivery to cervical spinal cord is a promising therapeutic strategy, particularly because of it relevance to addressing respiratory compromise associated with ALS. Over the last 10 years, accumulating data has implicated non-neuronal cells in the pathogenesis of neuronal degeneration in ALS. Starting from the earliest observation of functional abnormalities in ALS astrocytes18,28 to the more recent studies in chimeric mice8, the aberrant function of cells, including microglia7 and astroglia13, that surround motor neuron somas and dendrites appears to contribute to disease progression. Chimeric mutant SOD1 expression models suggest that increasing the proportion of healthy wild-type non-neuronal cells is inversely related to measures of disease severity such as animal survival8, similar to the GRP transplantation effects presented in the current study. In these chimeric animals, the presence of wild-type non-neuronal cells (likely astrocytes and microglia) in the spatial vicinity of mutant SOD1 expressing motor neurons prevents pathological changes in these neurons. More recent studies demonstrate that the reduction of mutant SOD1 selectively from astrocytes using $LoxSOD1^{G37R}$ / $GFAP\text{-}Cre^{+}$ mice results in a prolongation of disease duration, but has no effects on disease onset13. These results suggest a particular role for astrocytes in later progression of disease. In aggregate, these studies suggest that replacement of abnormal astroglia - or enrichment of healthy astroglia - with normal functioning precursors, could be one approach towards focally altering the microenvironment around motor neurons.

Dysfunction of astrocyte glutamate transport, specifically GLT1 (EAAT2), is found in humans with ALS and in animal models of ALS6,18, and may be a contributing factor in disease progression. Loss of this astroglial protein is known to cause excitotoxic motor neuron degeneration15. Furthermore, ALS astrocytes alter the expression of motor neuron dendritic glutamate (AMPA) receptors, also making them more susceptible to excitotoxicity. Small molecule drug screening for agents that enhance glial glutamate transporter function shows that increasing astroglial GLT1 can be beneficial in ALS models29. More recently, several in vitro studies of immature ALS rodent astrocytes also suggest abnormal properties resulting in motor neuron cell death9,11, although the exact mechanisms remain unknown. Thus, any approach to offset or replace altered astroglial function - especially in mature astrocytes - may be of therapeutic benefit.

In the current work, GRP transplants were able to partially prevent loss of total tissue GLT1 levels in cervical cord, thereby targeting one important, and ALS-relevant, function of astrocytes. The demonstration that $GLT1^{-/-}$ GRPs did not have any effects on behavioral measures or animal survival also suggests that glutamate-relevant pathways may contribute to the cascade of events leading to cell death in this model and that the focal beneficial effects of GRP transplantation could be explained, at least in part, by increases in glutamate transporter expression. While disease duration is extended by reducing mutant SOD1 from astrocytes in the $LoxSOD1^{G37R}$/GFAP-Cre^{+} mice, GLT1 loss in lumbar spinal cord sections is not dependent on the presence of mutant SOD1 in astrocytes13. GLT1 loss may instead be related to non-cell autonomous damage to astrocytes from SOD1 synthesis by other cells. Alternatively, alterations in neuron-astrocyte communication, as a result of SOD1-mediated neuronal injury, could be responsible. Several possible explanations could account for the discrepancy between the current observations and the previous study13. These include the anatomical location of tissue sampling (both cervical and lumbar spinal cord versus lumbar only), time frame of sampling (at a specific time point during disease course versus end-stage), as well as the contributions of GLT1 loss to death in different species carrying different SOD1 mutations that result in differences in disease course itself (less than 180 days in the $SOD1^{G93A}$ rat model versus greater that 375 days in the $SOD1^{G37R}$ mouse model). Finally, it is also possible that the increases in GLT1 that we observed in our model may represent only one of several related pathways relevant to astrocytic influences on disease progression. The lack of further increases in behavioral and neuroprotective measures from the transplantation of GLT1-overexpressing GRPs may be related to the observation that increases in GLT1 levels were relatively small compared to previous in vitro studies24 and in vivo drug studies29.

Astrogliosis with GFAP up-regulation is a central feature of ALS and SOD1 pathology, and previous studies have noted that some protective molecules down-regulate GFAP expression in ALS models30. We did not observe any detrimental effects on disease by the introduction of $GFAP^{+}$ GRP-derived astrocytes. These results suggest that astrogliosis may not only be reflected by increases in GFAP expression, but also by other astrocyte factors which may influence disease progression. Furthermore, the direct effect of astrogliosis itself is unclear as reactive astrocytes also play important protective roles in other CNS injury paradigms31.

Neural precursor cell transplantation offers a strategy for slowing neurodegenerative disease progression and/or promoting recovery of function because engrafted cells have the potential of replacing lost or dysfunctional neurons and glia. Previous neural precursor transplantation studies in motor neuronopathies have focused mostly on motor neuron replacement32–35; however, this is a challenging strategy for neurodegenerative diseases because of problems associated with motor neuron differentiation, establishment of appropriate circuitry with host neurons, and extension to and connectivity with musculature.

Other transplantation strategies not based on motor neuron replacement, including those with enhanced trophic factor production, also show promise in ALS models36–47. When transplanted into the lumbar spinal cord of $SOD1^{G93A}$ rats, human cortical NPCs that over-express the trophic factor, GDNF, provide some, albeit limited, neuroprotection48,49. These transplants provide a neuroprotective effect on motor neuron survival, but do not promote efficacy with respect to improved hind-limb motor performance and animal survival, possibly due to lack of astrocyte differentiation in vivo. Our study did not suggest that there was a pattern of significant increases in VEGF, IGF-1 or BDNF neurotrophic factor secretion to account for the observed pathological or behavioral phenotypes. However, it is possible that at the cellular level some neurotrophic factor secretion may have played a role in the efficacy of GRPs, but was not appreciated in the whole tissue analysis of the cervical spinal cord in this study.

These results serve as a proof-of-principle that stem cell transplantation-based astrocyte replacement is feasible and a potentially viable option for ALS therapy. Delivery to the cervical spinal cord targets key motor neuron pools which ultimately affect survival in ALS patients, and respiratory measures remain the most reliable for use in ALS clinical trials.

Glial precursors are particularly promising candidates for astrocyte replacement because of their robust survival, efficient astrocytic differentiation, and lack of tumor formation. While more immature cell classes such as multipotent neural stem cells and pluripotent embryonic stem cells are desirable sources for transplant derivation, the current work suggests that the use of more mature lineage-restricted progenitors may be an optimal strategy for achieving targeted phenotypic replacement.

Materials and Methods

GRP Transplantation

GRPs, GLT1 over-expressing GRPs (“G3s”), $GLT1^{-/-}$ GRPs, freeze-thawed dead GRPs and unmodified rat fibroblasts25 were suspended at a concentration of 7.5×10^4 cells/uL (in basal media). Immune suppressed (cyclosporine A: 10mg/kg; Sandoz Pharmaceuticals, East Hanover, NJ) animals received transplants at 90 days of age. 7 groups of animals were used: wild-type rat GRPs, GLT1 over-expressing rat GRPs, $GLT1^{-/-}$ mouse GRPs, wild-type mouse GRPs, fibroblasts, dead (freeze-thawed) wild-type rat GRPs, media. Each rat received 6 grafts (bilaterally at C4, C5 and C6) of 1.5×10^5 cells (in 2uL basal media) into ventral horn. Briefly, cells were delivered using a 10uL Hamilton Gastight syringe (Hamilton) with an attached 30-gauge 45° beveled needle (Hamilton). The injection pipette was secured to a manual micromanipulator (World Precision Instruments; Sarasota, FL)

attached to an 80° tilting base. The tip was lowered to a depth of 1.5mm below the surface of the cord and was held in place for 2 minutes before and after cell injection. Cells were delivered under the control of a microsyringe pump controller (World Precision Instruments) at a rate of 0.5uL/minute.

Hind-limb and Fore-limb Grip Strength

Animal weighing and all behavioral data collection began 1 week prior to transplantation, and was conducted twice weekly until end-stage. Hind- and fore-limb muscle grip strengths were separately determined using a "Grip Strength Meter" (DFIS-2 Series Digital Force Gauge; Columbus Instruments, OH).

Disease Onset

Hind- and fore-limb disease onsets were assessed individually for each rat by a 20.0% loss in hind- or fore-limb grip strength relative to each animal's own baseline grip strength level.

Survival/Endstage Analysis

To determine disease end-stage in a reliable and ethical fashion, end-stage was defined by the inability of rats to right themselves within 30 seconds when placed on their sides.

Disease Duration

Overall onset of disease was determined by hind-limb grip strength onset because hind-limb deficits are the first clinical symptoms observed in most rats. Disease duration was measured as time between hind-limb disease onset and disease end-stage. All $SOD1^{G93A}$ animals were included in overall survival, disease onset and grip strength analyses; however, rats that displayed fore-limb onset prior to hind-limb onset (approximately 10% of $SOD1^{G93A}$ rats) were excluded from disease duration analysis, as well as from analysis of the delay of fore-limb onset following hind-limb onset.

Fore-limb/Hind-limb Combined Motor Score

A 5-point scale was used to simultaneously assess fore- and hind-limb function, as previously described47.

Compound Muscle Action Potential (CMAP) Recordings

Under anesthesia, phrenic nerve conduction studies were performed21 with stimulation (0.5 ms single stimulus; 1 Hz supramaximal pulses) at the neck via near nerve needle electrodes placed 0.5 cm apart along the phrenic nerve. Recording was obtained via a surface strip along the costal margin, and CMAP amplitude was measured baseline to peak. Recordings across the nerve segment were made using an ADI Powerlab 8SP stimulator and BioAMP amplifier (Powerlab), followed by computer assisted data analysis (Scope 3.5.6; ADI). Distal motor latency of evoked potentials includes duration of nerve conduction between stimulating and recording electrodes plus time of synaptic transmission.

Statistical Analysis

Kaplan-Meier analysis of the $SOD1^{G93A}$ rats was conducted using the statistical software Sigmastat (SAS Software) to analyze survival, disease onset and duration data. Weight and grip strength results were analyzed via ANOVA. In some cases, Student *t-test* was performed to compare data between groups of animals. All data are presented as mean ± S.E.M., and significance level was set at $p \leq 0.05$.

Supplementary Material

Refer to Web version on PubMed Central for supplementary material.

Acknowledgements

We thank: all members of the Maragakis and Rothstein labs for helpful discussion; The Robert Packard Center for ALS Research (N.J.M.), The ALS Association (N.J.M.) and the NIH (F32-NS059155: A.C.L., R01-NS33958: J.D.R. and R01-NS41680: J.D.R. and N.J.M.) for funding; K Tanaka for providing $GLT1^{-/-}$ mice.

Literature Cited

1. Bruijn LI, Miller TM, Cleveland DW. Unraveling the mechanisms involved in motor neuron degeneration in ALS. Annu Rev Neurosci. 2004; 27:723–749. [PubMed: 15217349]
2. Rosen DR, et al. Mutations in Cu/Zn superoxide dismutase gene are associated with familial amyotrophic lateral sclerosis. Nature. 1993; 362:59–62. [PubMed: 8446170]
3. Bruijn LI, et al. ALS-linked SOD1 mutant G85R mediates damage to astrocytes and promotes rapidly progressive disease with SOD1-containing inclusions. Neuron. 1997; 18:327–338. [PubMed: 9052802]
4. Gurney ME, et al. Motor neuron degeneration in mice that express a human Cu,Zn superoxide dismutase mutation. Science. 1994; 264:1772–1775. [PubMed: 8209258]
5. Wong PC, et al. An adverse property of a familial ALS-linked SOD1 mutation causes motor neuron disease characterized by vacuolar degeneration of mitochondria. Neuron. 1995; 14:1105–1116. [PubMed: 7605627]
6. Howland DS, et al. Focal loss of the glutamate transporter EAAT2 in a transgenic rat model of SOD1 mutant-mediated amyotrophic lateral sclerosis (ALS). Proc Natl Acad Sci U S A. 2002; 99:1604–1609. [PubMed: 11818550]
7. Boillee S, et al. Onset and progression in inherited ALS determined by motor neurons and microglia. Science. 2006; 312:1389–1392. [PubMed: 16741123]
8. Clement AM, et al. Wild-type nonneuronal cells extend survival of SOD1 mutant motor neurons in ALS mice. Science. 2003; 302:113–117. [PubMed: 14526083]
9. Di Giorgio FP, Carrasco MA, Siao MC, Maniatis T, Eggan K. Non-cell autonomous effect of glia on motor neurons in an embryonic stem cell-based ALS model. Nat Neurosci. 2007; 10:608–614. [PubMed: 17435754]
10. Lino MM, Schneider C, Caroni P. Accumulation of SOD1 mutants in postnatal motoneurons does not cause motoneuron pathology or motoneuron disease. J Neurosci. 2002; 22:4825–4832. [PubMed: 12077179]
11. Nagai M, et al. Astrocytes expressing ALS-linked mutated SOD1 release factors selectively toxic to motor neurons. Nat Neurosci. 2007; 10:615–622. [PubMed: 17435755]
12. Pramatarova A, Laganiere J, Roussel J, Brisebois K, Rouleau GA. Neuron-specific expression of mutant superoxide dismutase 1 in transgenic mice does not lead to motor impairment. J Neurosci. 2001; 21:3369–3374. [PubMed: 11331366]
13. Yamanaka K, et al. Astrocytes as determinants of disease progression in inherited amyotrophic lateral sclerosis. Nat Neurosci. 2008; 11:251–253. [PubMed: 18246065]

14. Pekny M, Nilsson M. Astrocyte activation and reactive gliosis. Glia. 2005; 50:427–434. [PubMed: 15846805]
15. Rothstein JD, et al. Knockout of glutamate transporters reveals a major role for astroglial transport in excitotoxicity and clearance of glutamate. Neuron. 1996; 16:675–686. [PubMed: 8785064]
16. Rothstein JD, et al. Localization of neuronal and glial glutamate transporters. Neuron. 1994; 13:713–725. [PubMed: 7917301]
17. Maragakis NJ, Rothstein JD. Mechanisms of Disease: astrocytes in neurodegenerative disease. Nat Clin Pract Neurol. 2006; 2:679–689. [PubMed: 17117171]
18. Rothstein JD, Van Kammen M, Levey AI, Martin LJ, Kuncl RW. Selective loss of glial glutamate transporter GLT-1 in amyotrophic lateral sclerosis. Ann Neurol. 1995; 38:73–84. [PubMed: 7611729]
19. Rao MS, Mayer-Proschel M. Glial-restricted precursors are derived from multipotent neuroepithelial stem cells. Dev Biol. 1997; 188:48–63. [PubMed: 9245511]
20. Rao MS, Noble M, Mayer-Proschel M. A tripotential glial precursor cell is present in the developing spinal cord. Proc Natl Acad Sci U S A. 1998; 95:3996–4001. [PubMed: 9520481]
21. Llado J, et al. Degeneration of respiratory motor neurons in the SOD1 G93A transgenic rat model of ALS. Neurobiol Dis. 2006; 21:110–118. [PubMed: 16084734]
22. Tankersley CG, Haenggeli C, Rothstein JD. Respiratory impairment in a mouse model of amyotrophic lateral sclerosis. J Appl Physiol. 2007; 102:926–932. [PubMed: 17110520]
23. Matsumoto A, et al. Disease progression of human SOD1 (G93A) transgenic ALS model rats. J Neurosci Res. 2006; 83:119–133. [PubMed: 16342121]
24. Maragakis NJ, et al. Glial restricted precursors protect against chronic glutamate neurotoxicity of motor neurons in vitro. Glia. 2005; 50:145–159. [PubMed: 15657939]
25. Mitsui T, Fischer I, Shumsky JS, Murray M. Transplants of fibroblasts expressing BDNF and NT-3 promote recovery of bladder and hindlimb function following spinal contusion injury in rats. Exp Neurol. 2005; 194:410–431. [PubMed: 16022868]
26. Maragakis NJ, Rothstein JD. Glutamate transporters: animal models to neurologic disease. Neurobiol Dis. 2004; 15:461–473. [PubMed: 15056453]
27. Federici T, Boulis NM. Gene-based treatment of motor neuron diseases. Muscle Nerve. 2006; 33:302–323. [PubMed: 16228969]
28. Rothstein JD, Martin LJ, Kuncl RW. Decreased glutamate transport by the brain and spinal cord in amyotrophic lateral sclerosis. N Engl J Med. 1992; 326:1464–1468. [PubMed: 1349424]
29. Rothstein JD, et al. Beta-lactam antibiotics offer neuroprotection by increasing glutamate transporter expression. Nature. 2005; 433:73–77. [PubMed: 15635412]
30. Kiaei M, Kipiani K, Chen J, Calingasan NY, Beal MF. Peroxisome proliferator-activated receptor-gamma agonist extends survival in transgenic mouse model of amyotrophic lateral sclerosis. Exp Neurol. 2005; 191:331–336. [PubMed: 15649489]
31. Sofroniew MV. Reactive astrocytes in neural repair and protection. Neuroscientist. 2005; 11:400–407. [PubMed: 16151042]
32. Deshpande DM, et al. Recovery from paralysis in adult rats using embryonic stem cells. Ann Neurol. 2006; 60:32–44. [PubMed: 16802299]
33. Harper JM, et al. Axonal growth of embryonic stem cell-derived motoneurons in vitro and in motoneuron-injured adult rats. Proc Natl Acad Sci U S A. 2004; 101:7123–7128. [PubMed: 15118094]
34. Kerr DA, et al. Human embryonic germ cell derivatives facilitate motor recovery of rats with diffuse motor neuron injury. J Neurosci. 2003; 23:5131–5140. [PubMed: 12832537]
35. Wu P, et al. Region-specific generation of cholinergic neurons from fetal human neural stem cells grafted in adult rats. Nature Neuroscience. 2002; 5:1271–1278. [PubMed: 12426573]
36. Aebischer P, et al. Gene therapy for amyotrophic lateral sclerosis (ALS) using a polymer encapsulated xenogenic cell line engineered to secrete hCNTF. Hum Gene Ther. 1996; 7:851–860. [PubMed: 8860837]

37. Aebischer P, et al. Intrathecal delivery of CNTF using encapsulated genetically modified xenogeneic cells in amyotrophic lateral sclerosis patients. Nat Med. 1996; 2:696–699. [PubMed: 8640564]
38. Corti S, et al. Wild-type bone marrow cells ameliorate the phenotype of SOD1-G93A ALS mice and contribute to CNS, heart and skeletal muscle tissues. Brain. 2004; 127:2518–2532. [PubMed: 15469951]
39. Corti S, et al. Neural stem cells LewisX+ CXCR4+ modify disease progression in an amyotrophic lateral sclerosis model. Brain. 2007; 130:1289–1305. [PubMed: 17439986]
40. Garbuzova-Davis S, et al. Intraspinal implantation of hNT neurons into SOD1 mice with apparent motor deficit. Amyotroph Lateral Scler Other Motor Neuron Disord. 2001; 2:175–180. [PubMed: 11958728]
41. Garbuzova-Davis S, et al. Positive effect of transplantation of hNT neurons (NTera 2/D1 cell-line) in a model of familial amyotrophic lateral sclerosis. Exp Neurol. 2002; 174:169–180. [PubMed: 11922659]
42. Garbuzova-Davis S, et al. Intravenous administration of human umbilical cord blood cells in a mouse model of amyotrophic lateral sclerosis: distribution, migration, and differentiation. J Hematother Stem Cell Res. 2003; 12:255–270. [PubMed: 12857367]
43. Hemendinger R, et al. Sertoli cells improve survival of motor neurons in SOD1 transgenic mice, a model of amyotrophic lateral sclerosis. Exp Neurol. 2005; 196:235–243. [PubMed: 16242126]
44. Llado J, Haenggeli C, Maragakis NJ, Snyder EY, Rothstein JD. Neural stem cells protect against glutamate-induced excitotoxicity and promote survival of injured motor neurons through the secretion of neurotrophic factors. Mol Cell Neurosci. 2004; 27:322–331. [PubMed: 15519246]
45. Martin LJ, Liu Z. Adult olfactory bulb neural precursor cell grafts provide temporary protection from motor neuron degeneration, improve motor function, and extend survival in amyotrophic lateral sclerosis mice. J Neuropathol Exp Neurol. 2007; 66:1002–1018. [PubMed: 17984682]
46. Xu L, et al. Human neural stem cell grafts ameliorate motor neuron disease in SOD-1 transgenic rats. Transplantation. 2006; 82:865–875. [PubMed: 17038899]
47. Yan J, et al. Combined immunosuppressive agents or CD4 antibodies prolong survival of human neural stem cell grafts and improve disease outcomes in amyotrophic lateral sclerosis transgenic mice. Stem Cells. 2006; 24:1976–1985. [PubMed: 16644922]
48. Klein SM, et al. GDNF delivery using human neural progenitor cells in a rat model of ALS. Hum Gene Ther. 2005; 16:509–521. [PubMed: 15871682]
49. Suzuki M, et al. GDNF secreting human neural progenitor cells protect dying motor neurons, but not their projection to muscle, in a rat model of familial ALS. PLoS ONE. 2007; 2:e689. [PubMed: 17668067]

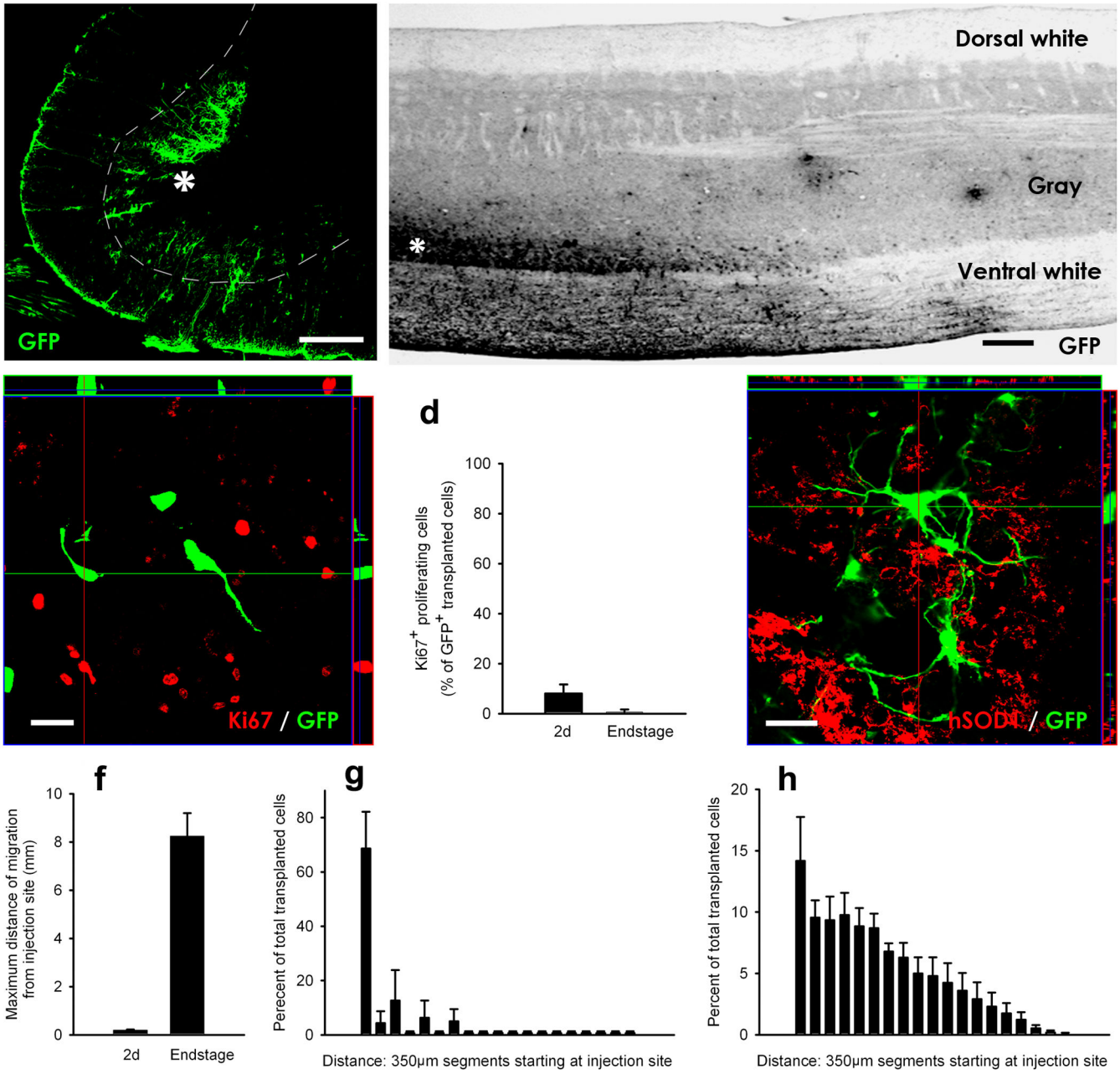

Figure 1. GRP transplants robustly survived and migrated in the cervical spinal cord in SOD1^{G93A} rats

GRP transplants robustly survived in gray (a–b) and white (b) matter regions of cervical spinal cord at disease end-stage. Transplants were located in both ventral gray matter (a–b) and surrounding white matter (b) regions at sites of injection (asterisk), and migrated away from injection sites in both rostral and caudal directions along white matter tracts (b). The vast majority of transplanted cells did not express the proliferation marker, Ki67, in vivo at 2 days post-transplantation (c). Quantification shows that only a small percentage of GFP$^+$ cells expressed Ki67 at 2 days post-transplantation, while no transplant proliferation occurred at disease end-stage (d). GFP$^+$ transplants did not fuse with host human SOD1$^+$

cells (e). Quantification of GRP migration revealed that at 2 days post-engraftment transplanted cells were found on average no farther than 0.19mm from the injection site, while GRPs had migrated up to 8.3mm from the injection site at disease end-stage (f). Histograms depicting the percentage of cells at various distances from sites of injection show that the migratory patterns of transplants in gray versus white matter were distinct. The vast majority of cells were located close to the injection site in gray matter (g). In white matter, the highest proportion of cells was located close to the injection, and the location of cells gradually tapered away with increased distance (h). Scale bars: 200μm (a–b), 20um (c, e).Error bars: s.e.m.

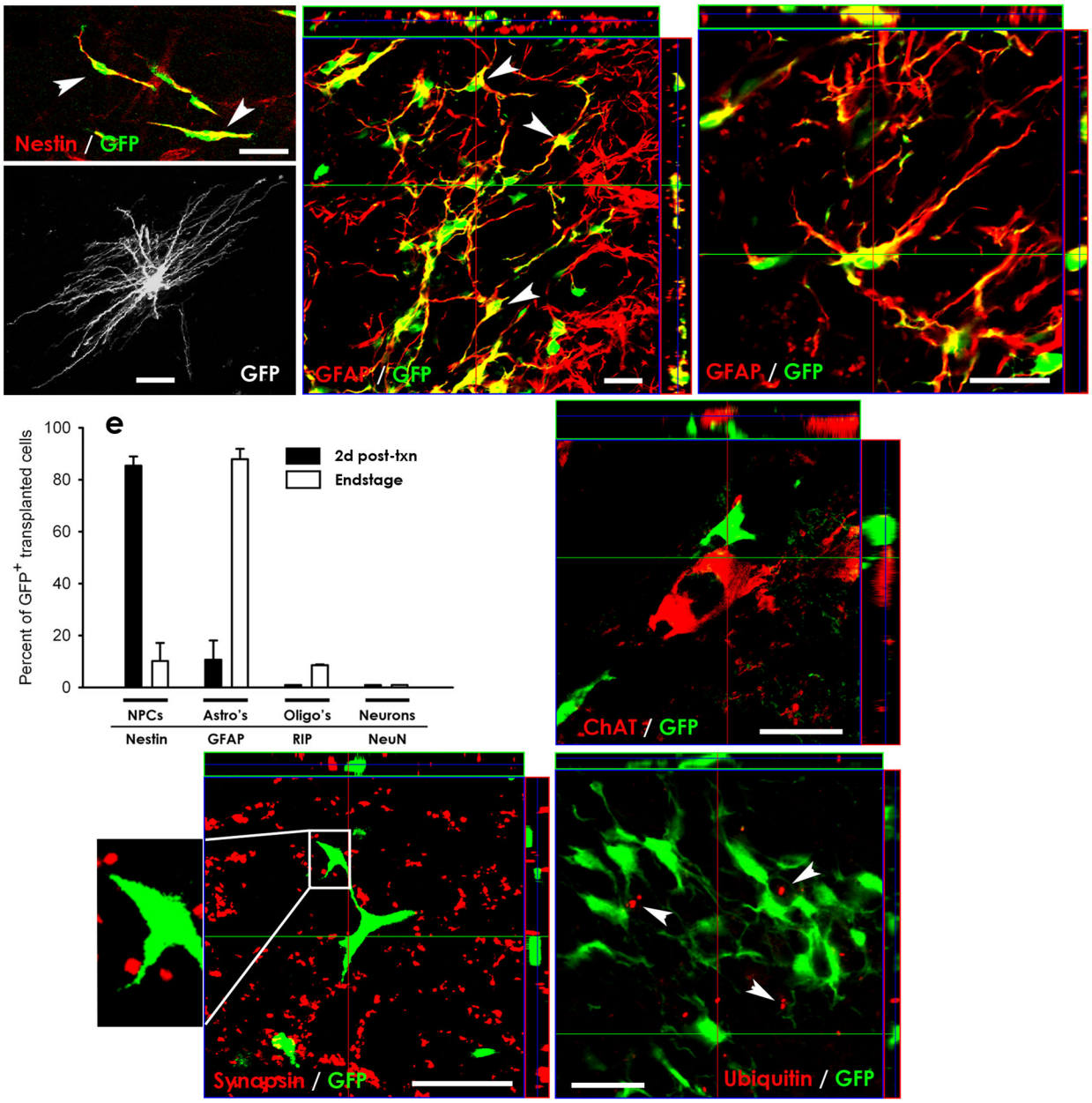

Figure 2. GRP transplants efficiently differentiated into astrocytes and spatially interacted with host ventral horn motor neurons in SOD1^{G93A} cervical spinal cord

Initially following transplantation, the vast majority of transplanted GFP$^+$ cells were still nestin$^+$ GRPs (arrowheads) (a). At end-stage, GFP$^+$ GRPs efficiently differentiated into GFAP$^+$ astrocytes following transplantation (c–d), and elaborated mature astrocytic morphologies (b). Quantification of the differentiation profile of transplanted GRPs at 2 days post-transplantation and at disease end-stage depicts the efficient transition from immature to mature phenotypes in vivo (e). Transplanted GFP$^+$ cells came into close direct contact with cell bodies of host ChAT$^+$ motor neurons (f) and with synapsin$^+$ synaptic sites (g: boxed area is shown at higher magnification) within ventral horn. Extensive ubiquitin deposition (arrowheads) was found in host cervical spinal cord cells at disease end-stage (h).

However, only rare transplanted GFP^+ cells contained such ubiquitin aggregates, suggesting that transplanted cells did not succumb to a similar pathological fate as host astrocytes in response to disease. Scale bars: 25μm. Error bars: s.e.m.

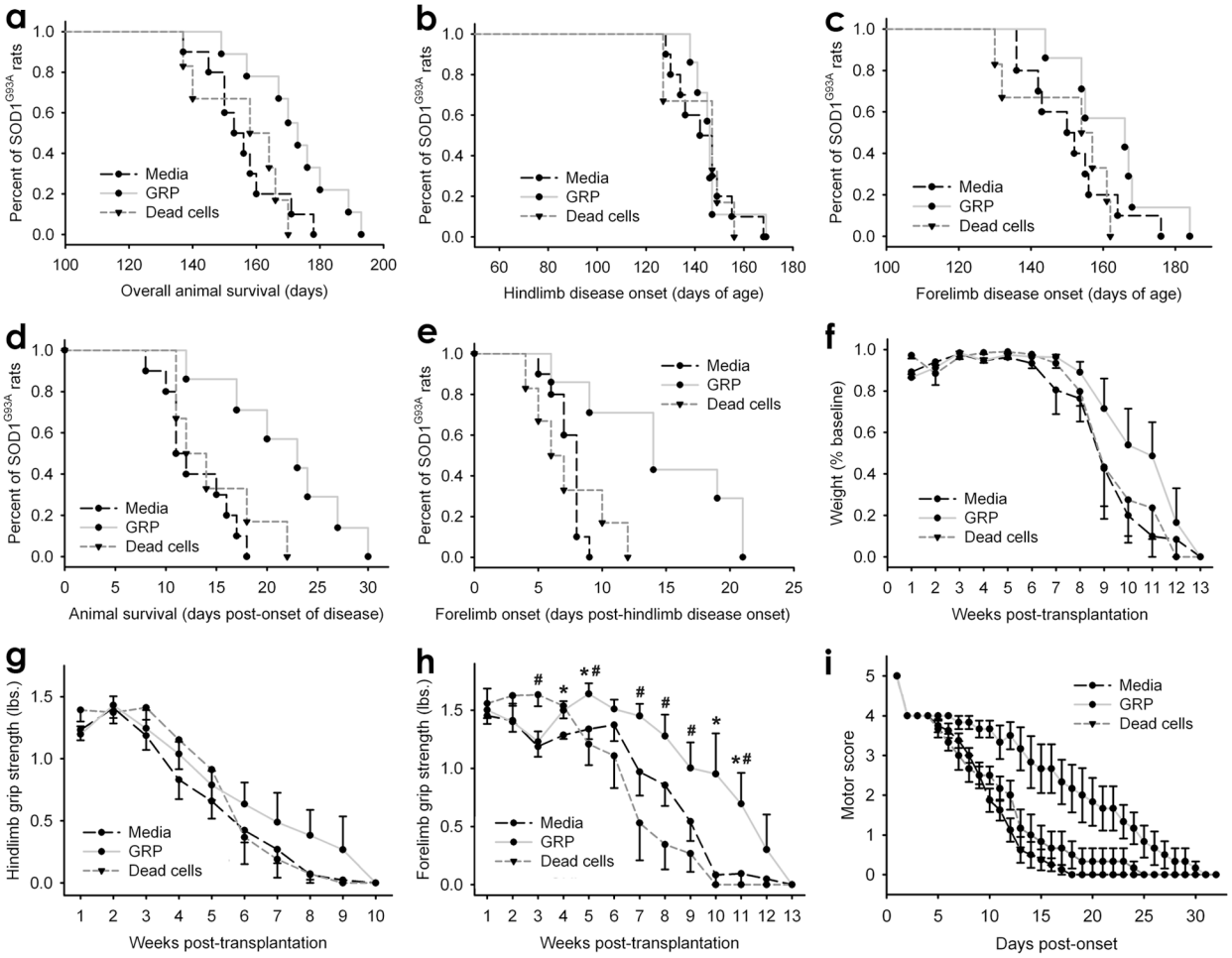

Figure 3. Following transplantation into cervical spinal cord of SOD1^{G93A} rats, GRP transplants extended survival and disease duration, and slowed declines in forelimb grip strength and motor performance

Compared to injection of media or dead cells, GRP transplants significantly increased overall animal survival (a). GRPs had no effect on hind-limb disease onset (b), but promoted a trend towards a delay in fore-limb onset (c). Disease duration was significantly prolonged by GRPs (d). A significant increase in the delay to fore-limb disease onset following hind-limb onset was observed in GRP transplanted animals (e). GRPs did not significantly delay weight decline (f). GRPs significantly delayed decline in fore-limb grip strength (h; * media vs GRPs;# dead cells vs GRPs), but had no effect on the rate of hind-limb grip strength decline (g). GRPs also slowed decline in motor performance (i). Error bars: s.e.m.

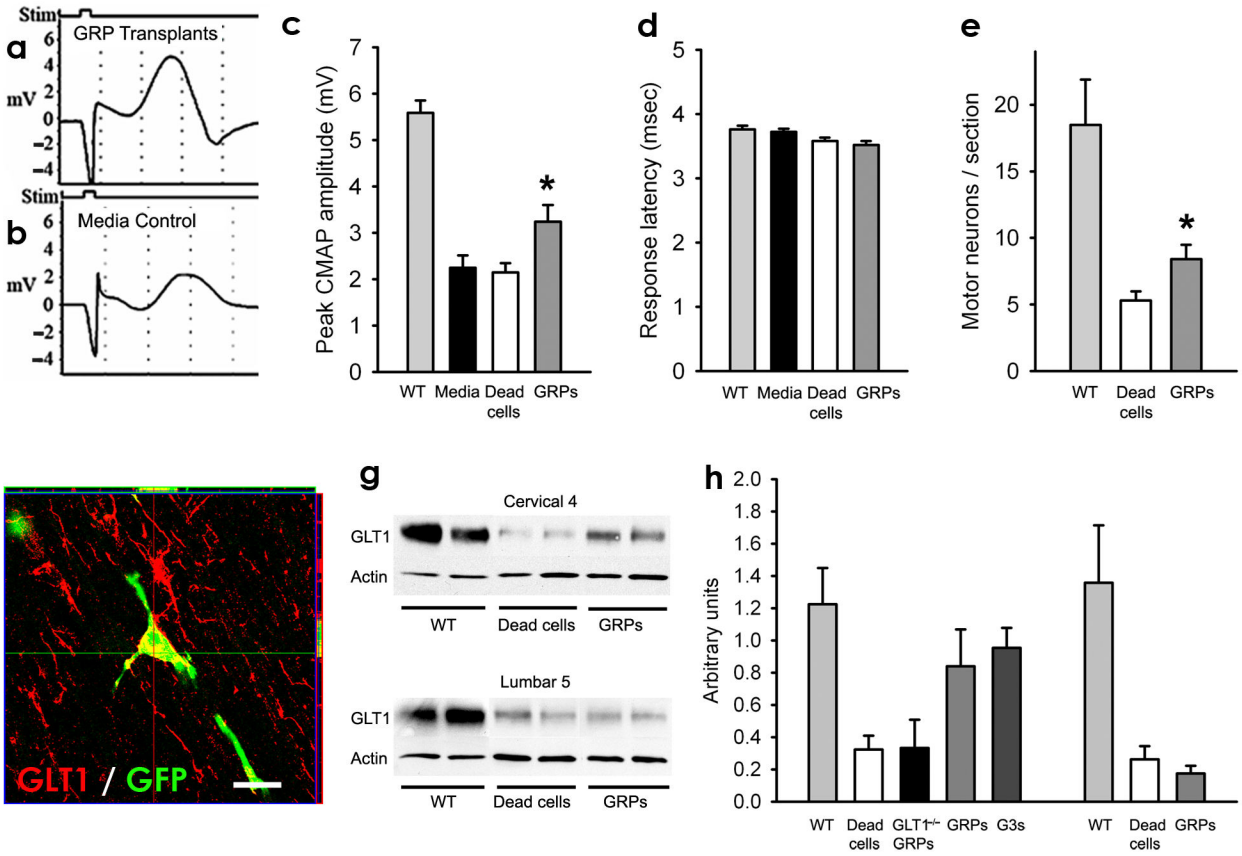

Figure 4. Following transplantation into cervical spinal cord of SOD1^{G93A} rats, GRP transplants partially slowed cervical spinal cord motor neuron and GLT1 protein loss, as well as decline in phrenic nerve compound muscle action potentials (CMAPs)

Compared to age-matched wild-type rats, all groups of SOD1^{G93A} rats had significantly reduced peak response amplitudes in phrenic nerve CMAPs, an electrophysiological measure of diaphragm function (c). CMAPs (a–b) were recorded at 8 days post hind-limb disease onset, and a significant increase (c) in peak response amplitude was found in GRP transplanted rats. GRPs had no effect on latency of response (d). Compared to age-matched wild-type rats, all groups of SOD1^{G93A} rats had significantly reduced numbers of cervical spinal cord motor neurons (e). Compared to dead cell control, GRPs partially rescued cervical motor neurons (e). Grafted GFP^{+} cells continued to express GLT1 protein at disease endstage (f). Compared to age-matched wild-type rats, all groups of SOD1^{G93A} rats had reduced levels of total GLT1 protein at C4 (g). Compared to dead cell control and GLT1$^{-/-}$ GRP transplants, GRP and GLT1 over-expressing GRP (G3s) transplants had higher levels of total GLT1 levels at C4 (h). There was no difference in C4 GLT1 levels between GRPs and GLT1 over-expressing GRPs (h). However, no differences in total GLT1 protein amongst any of the treatment groups were found at L5 (g, h), demonstrating that focal transplantation resulted in changes in transporter protein levels only at cervical regions and that disease progression was likely occurring unchanged at other non-targeted areas. Scale bars: 20μm. Error bars: s.e.m.

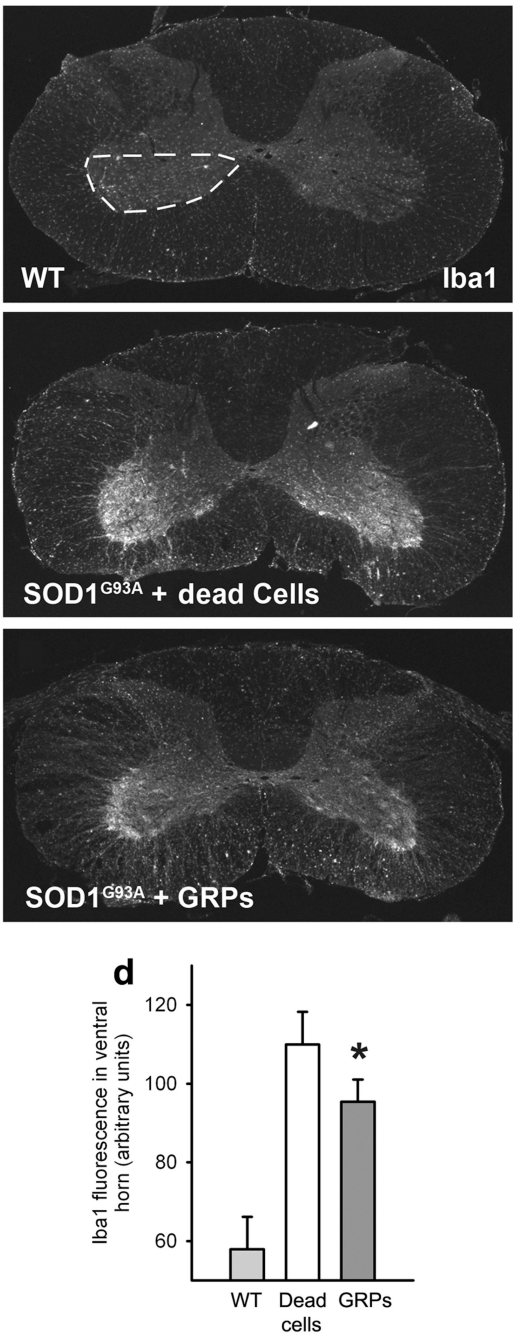

Figure 5. GRP transplants decreased ventral horn microgliosis

Compared to wild-type spinal cord (a), there was a significantly elevated Iba1^{+} microglial response specifically in the ventral gray matter of SOD1^{G93A} rats with either media (b) or GRP (c) transplants. Quantification of the Iba1 response in ventral gray matter (denoted by region within dotted line) reveals that microgliosis was significantly reduced in GRP transplanted animals compared to media controls (d). Scale bars: 200μm. Error bars: s.e.m.